Combust. Sci. and Tech., 1988, Vol. 61, pp. 169–185
Reprints available directly from the publisher
Photocopying permitted by license only

Mechanisms Governing Transients from the Batch Incineration of Liquid Wastes in Rotary Kilns

JOST O. L. WENDT *Department of Chemical Engineering, University of Arizona, Tucson, AZ 85721 USA*

WILLIAM P. LINAK *Combustion Research Branch, MD-65, Air and Energy Engineering Research Laboratory, U.S. Environmental Protection Agency, Research Triangle Park, NC 27711, USA*

(Received April 18, 1988; in final form July 5, 1988)

Abstract—When "containerized" liquid wastes, bound on sorbents, are introduced into a rotary kiln in a batch mode, transient phenomena involving heat transfer into, and waste mass transfer out of, the sorbent can promote the rapid release of waste vapor into the kiln environment. This rapid vapor release can cause depletion and displacement of the excess oxygen from the primary flame, and formation of a "puff," which can result in a temporary failure of the incinerator system. Parametric studies on a specially designed rotary kiln incinerator simulator showed that puffs are easily generated even with very small quantities of surrogate wastes and at excess air values exceeding 100 percent. Furthermore, their magnitudes and intensities increase with increasing kiln temperature and kiln rotation speed.

A theoretical model describing simultaneous heat and mass transfer through a sorbent aggregate, coupled with vapor pressure driven waste vaporization within the sorbent aggregate, was combined with a fragmentation model and was able qualitatively to predict experimentally observed effects relating to puff duration, kiln rotation speed, kiln temperature, and stoichiometric oxygen requirement of the surrogate waste. Extrapolation of the model to conditions beyond the experimental test matrix indicated very strong influences of waste boiling point (and consequently latent heat), and of sorbent parameters such as overall void fraction in the container and the sorption characteristics of the individual sorbent particles. The theoretical results support the experimental data from the rotary kiln incinerator simulator and suggest that the experimentally observed trends have general practical validity. The model constitutes a first step in being able to rank wastes and sorbents with respect to their propensity to produce puffs.

NOMENCLATURE

C	Concentration in interstitial gas phase (gmole/cm^3)
C_0	Initial concentration in interstitial gas phase (gmole/cm^3)
C_{crit}	Critical concentration defining falling drying rate (gmole/cm^3 sorbent)
C_s	Concentration in sorbent (gmole/cm^3 sorbent)
C_{s0}	Initial concentration in sorbent (gmole/cm^3 sorbent)
C_p	Specific heat of sorbent (cal/g K)
d_g	Sorbent grain diameter (cm)
D_i	Aggregate diameter (cm)
D_{eff}	Effective diffusivity (cm^2/s)
D_m	Molecular diffusivity (cm^2/s)
F_f	Molar flow of flue gas (gmole/s)
F_w	Mass flow of waste out of surface (g/s)
ΔH_v	Waste latent heat of vaporization (cal/gmole)
i	Fragmentation event i
k	Thermal conductivity of sorbent (cal/s cm K)
k_1	Fragmentation constant
k_1'	Fragmentation constant (related to k_1)
k_2	Fragmentation constant
MASS	Charge mass (g)

MW	Molecular weight (g/gmole)
N_A	Molar flux of waste at sorbent aggregate surface (gmole/cm^2 s)
P/P_{base}	Relative puff magnitude (puff magnitude normalized by base case puff magnitude)
P^{vap}	Vapor pressure of waste (atm)
$Q(t)$	Heat flux into sorbent aggregate (cal/cm^2 s)
R_v	Vaporization rate (gmole/cm^3 s)
R	Gas constant (82.1 atm cm^3/gmole K)
RPM	Kiln rotation speed (rpm)
$S(D_i, t)$	Fragmentation rate (events/s)
T	Temperature (K)
T_0	Initial temperature (K)
T_b	Normal boiling point (K)
T_K	Kiln temperature (K)
T_M	Measured temperature at kiln exit (K)
t	Time (s)
Δt_i	Time interval between i'th and $i + 1$'th fragmentation event (s)
$W(t)$	Mass flux out of sorbent aggregate (g/cm^2 s)
y	Distance into sorbent aggregate (cm)
Y_{O_2}	Oxygen mole fraction after consuming evolved waste
$Y^0_{O_2}$	Oxygen mole fraction in primary flame flue gas

Greek Symbols

ε	Bulk porosity
ϱ	Sorbent density (g/cm^3)
ν	Stoichiometric oxygen requirement of waste (gmole O_2 required/g waste)

INTRODUCTION

In many practical rotary kiln applications involving the incineration of liquid wastes, combustion of the waste occurs in a batch mode rather than under steady-state conditions. In this batch mode of operation, the liquid waste, bound on sorbent material, is held in containers or drums, which are introduced one at a time into the incinerator. Upon entry into the incinerator, the container ruptures or burns, exposing the contents to the hot kiln environment. The liquid vaporizes rapidly and reacts with the excess oxygen present in the burned gases from the continuous primary flame. A possible kiln failure condition arises when the evolution of waste gases from the sorbent is more rapid than the rate at which the stoichiometric amount of oxygen can be supplied from the primary flame. This phenomenon, in the form of carbon monoxide excursions, has been observed to occur in full-scale rotary kiln incinerators (Bastian and Wood, 1987; Wood, 1987), and is important in practice.

The purpose of the research reported here was both to determine which waste, sorbent, and kiln parameters influenced the generation of puffs and to gain fundamental insight into why and how these parameters have the effects that they do. Therefore, the approach followed was first to conduct a statistically designed set of parametric experimental studies on a laboratory rotary kiln incinerator simulator, and second to relate the experimental results obtained to a mechanistic model which is based on known principles of heat and mass transfer. The latter can support the experimental studies by showing the general applicability of the results obtained, and can be extrapolated to conditions outside the experimental test matrix, while a purely empirical model cannot.

ROTARY KILN INCINERATOR SIMULATOR

Experimental results were obtained from the rotary kiln incinerator simulator shown on Figure 1. This 73 kW (250,000 Btu/h) prototype thermal destruction unit was designed to contain the salient features of practical kilns, but still be sufficiently versatile to allow parametric experimentation. This laboratory combustor has been described in detail elsewhere (Linak *et al.*, 1987a, 1987b). Since the results presented here are concerned solely with the transient phenomena occurring in the kiln itself, the afterburner (also shown in Figure 1) was not utilized. Internal diameter dimensions vary from 0.762 m (30 in.) in the kiln recess to 0.457 m (18 in.) in the afterburner and tower sections. Linak *et al.* (1987a) compared the design and operation of the simulator to full-scale units and concluded that this was a valid prototype experimental configuration and that results from this simulator did relate to full-scale units.

Surrogate waste materials are batch charged through the sliding gate/ram assembly illustrated in Figure 1. After a contained liquid charge is placed in the charging basket, the gate is opened and the basket is rammed into the kiln. At a set position, the basket is stopped and momentum carries the charge into the kiln. Upon destruction of the container walls, the charge, containing surrogate waste bound on sorbent, is exposed to the hot kiln environment. The surface exposed to this environmment appears to be controlled by the tumbling action prompted by the slow rotation speed of the kiln (0.5 to 2.0 rpm). The sorbent consisted of 135 g of ground corncob material, and completely filled a cylindrical, closed, uncoated, 0.95 litre (1 qt) cardboard container,

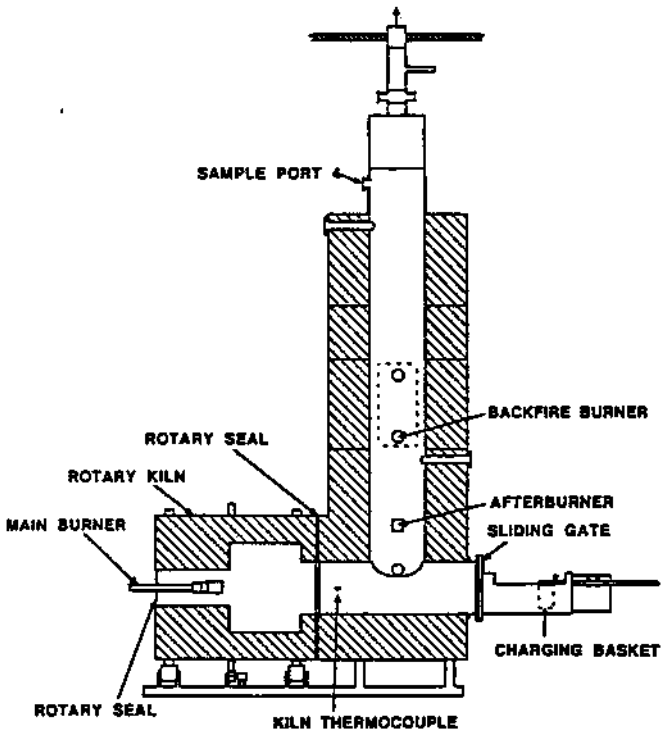

FIGURE 1 Rotary kiln incinerator simulator.

8.9 cm (3.5 in.) in diameter and 16.5 cm (6.5 in.) long, with a tare weight of 45 g. In contrast to other kiln applications (Zablotny, 1965), the aggregate of sorbent particles in this case fills only a tiny fraction of the kiln volume. The container with sorbent but no surrogate waste gave negligible low response background loadings.

Real-time sampling and analysis equipment is described by Linak *et al.* (1987a). In addition to real-time total volatile hydrocarbon (THC), CO, CO_2, O_2, and NO_x instrumental analyses, the soot loading collected on a filter in the analysis train was measured. At constant sample and stack gas flow rates, this quantity is proportional to the total integrated particulate loading in the puff. There are difficulties associated with the measurement of puff intensity and puff magnitude (Linak *et al.*, 1987b) since no single on-line measurement such as, for example THC, represented those quantities for all surrogate wastes, under all conditions examined. For toluene on sorbent, it was found that, while THC traces might represent puff intensities if these were low, the total filter sample representing total soot loading in the puff was a better indicator of puff magnitude over the entire range of conditions examined. For carbon tetrachloride on sorbent, CO was the best indicator, while THC seemed to be adequate for the less volatile No. 5 fuel oil. In this paper we focus on toluene, and therefore assume that THC traces properly represent instantaneous puff intensities provided these are relatively low, and that total filter loadings represent puff magnitudes (integrated puff intensities over the puff duration) over both low and high ranges. However, in view of the difficulties in obtaining quantitative experimental measurements of puff magnitudes, it seems reasonable, at this stage of model development, to aim for qualitative prediction of trends observed, rather than for absolute quantitative agreement between theory and data.

PARAMETRIC EXPERIMENTATION

The general methodology employed for the parametric studies was that of response surface experimentation (Hicks, 1973). This methodology permits determination, on the basis of one experiment involving a minimal number of trials, of an empirical relationship between the response and the controlled variables in the experimental design. Data on the dependent variables are collected at low, intermediate, and high settings of the independent variables, which were charge mass, kiln rotation speed, and kiln temperature. The temperature variable was that measured at the kiln exit, which can be correlated with the appropriate temperature within the kiln using the two measured (with suction pyrometer) temperature distributions (corresponding to high and low fire conditions) shown on Figure 2. The following kiln operating parameters were kept constant for all runs reported here:

(a) Auxiliary gas flow rate, 5.06 m^3/h (200 cfh).
(b) Air flow rate, 109.0 m^3/h (3850 cfh) leading to a constant stoichiometric ratio, SR, (defined as the inverse of the equivalence ratio) of 2.0.
(c) Burner position, −0.34 m (−13.5 in.) inside front kiln wall.
(d) Kiln pressure, −37.4 Pa (−0.15 in. H_2O).
(e) Sample port at position 4 (See Figure 1).

In the experiment, each trial consisted of between 5 and 15 replicate charges. The total area and peak height of the time-resolved traces of total hydrocarbon concentrations (THC), measured by flame ionization detection (FID), were recorded and are denoted as "peak area" and "peak height," respectively. Figure 3a shows a typical hydrocarbon trace for a charge consisting of 100 g of toluene on 135 g of corncob

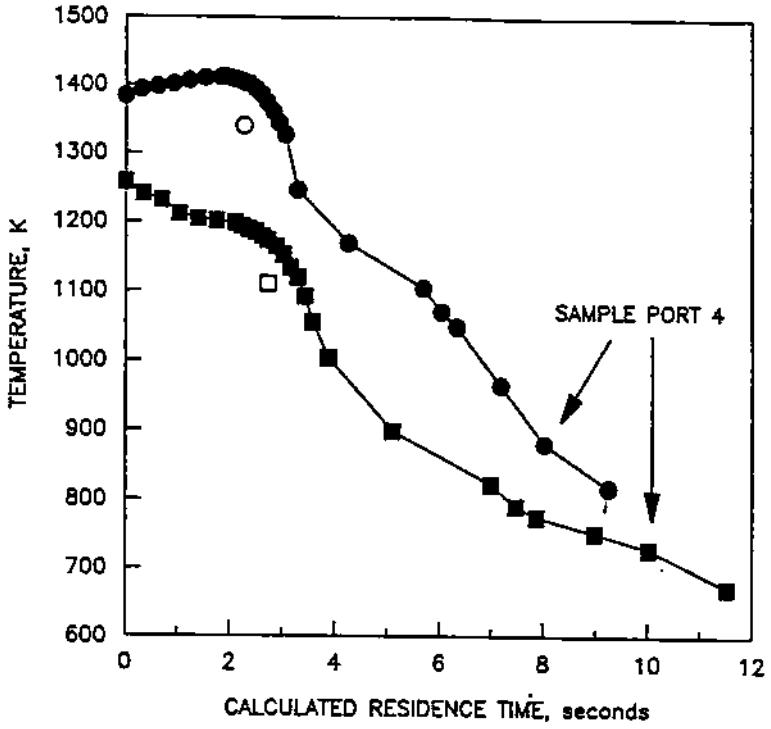

FIGURE 2 Measured temperature profile versus calculated residence time for □, ■ low-fire and ○, ● high-fire test conditions. Constant stoichiometric ratio (SR) = 2.0. Solid symbols indicate suction pyrometer temperatures. Open symbols indicate correlated thermocouple temperatures at kiln exit.

sorbent in a 0.95 litre (1 qt) closed cardboard container. Even though, at kiln temperatures, the vapor pressure of the liquid was exceeded by three or more orders of magnitude, the duration of each puff is prolonged over times exceeding 40 seconds, which is very much longer than would be the case if the liquid were injected without being bound on a sorbent. Note, furthermore, that the experimental trace (Figure 3a) consists of distinct multiple peaks even after the diffusion and mixing distortions arising from sampling. It is also significant that time resolved measurements of CO in the exhaust of full-scale rotary kiln incinerators showed spikes of similar durations (Bastian and Wood, 1987).

For toluene, both the area under the volatile hydrocarbon trace shown on Figure 3a and the weight of particulate matter collected on a filter were denoted as dependent response variables. Empirical quadratic models were fitted to the averaged data, using weighted least squares, where the weights were equal to the number of replicates divided by the sample variance between the replicates. Only statistically significant dependencies were retained in the model. These models were purely statistical, based on no mechanistic phenomena whatsoever, but they can be used to interpolate within the experimental test matrix, since they accounted for more than 99% of the variation in the response caused by changes in the independent parameters.

Experimental results depicting the effects of charge mass, kiln rotation speed, and kiln temperature on puff magnitude are shown on Figure 4. Puff magnitudes are measured by the weight of particulate matter collected on a filter, and are normalized by the value at "base case" conditions; namely: temperature, T_M (measured) = 1227 K, corresponding to T_K (kiln) = 1325 K; kiln rotation speed, RPM = 1.25; and charge

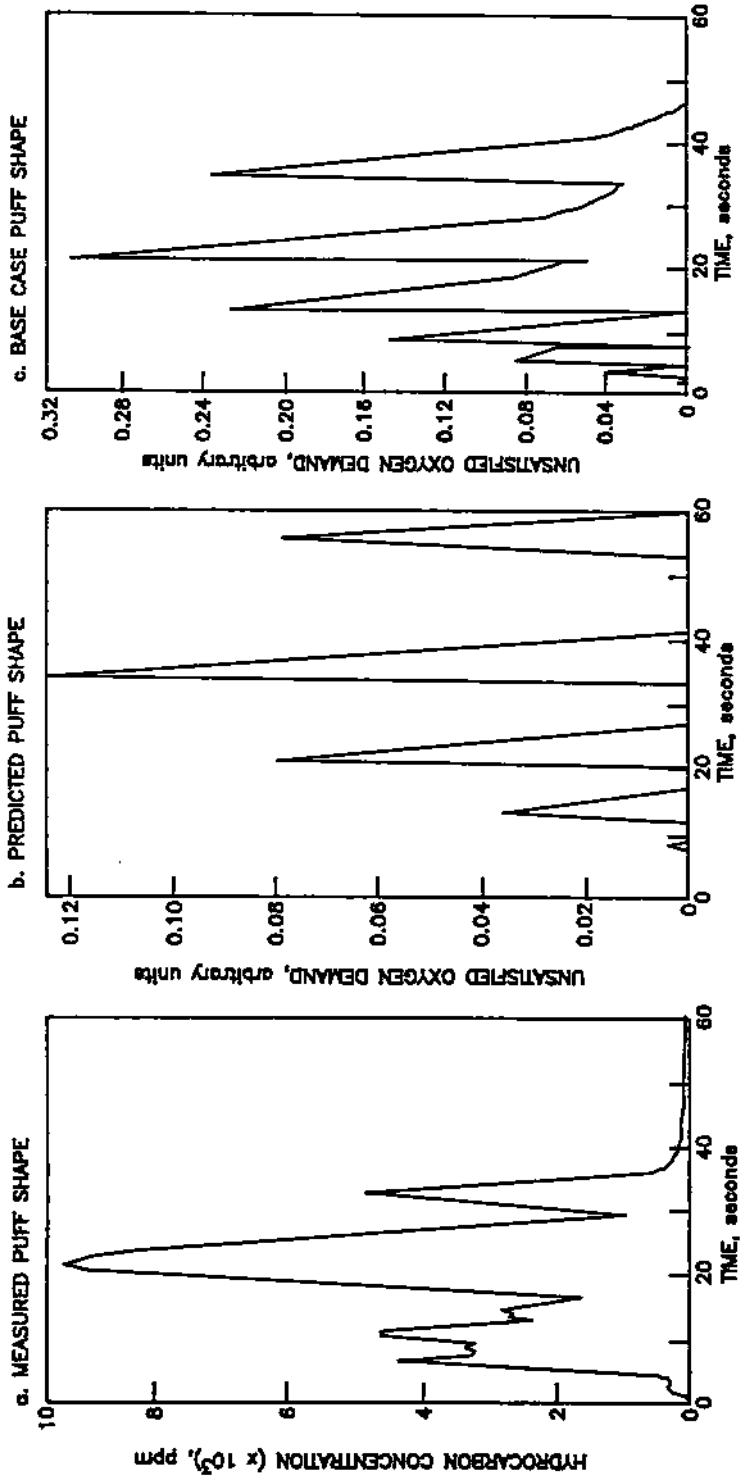

FIGURE 3 Measured and predicted toluene puff shapes. (a) Measured puff shape, MASS = 100 g, T_H = 1124 K (T_K = 1242 K), RPM = 0.5. (b) Predicted puff shape for case (a), MASS = 100 g, T_K = 1242 K, RPM = 0.5. (c) Predicted "base case" puff shape, MASS = 125 g, T_K = 1325 K, RPM = 1.25 (see Table I).

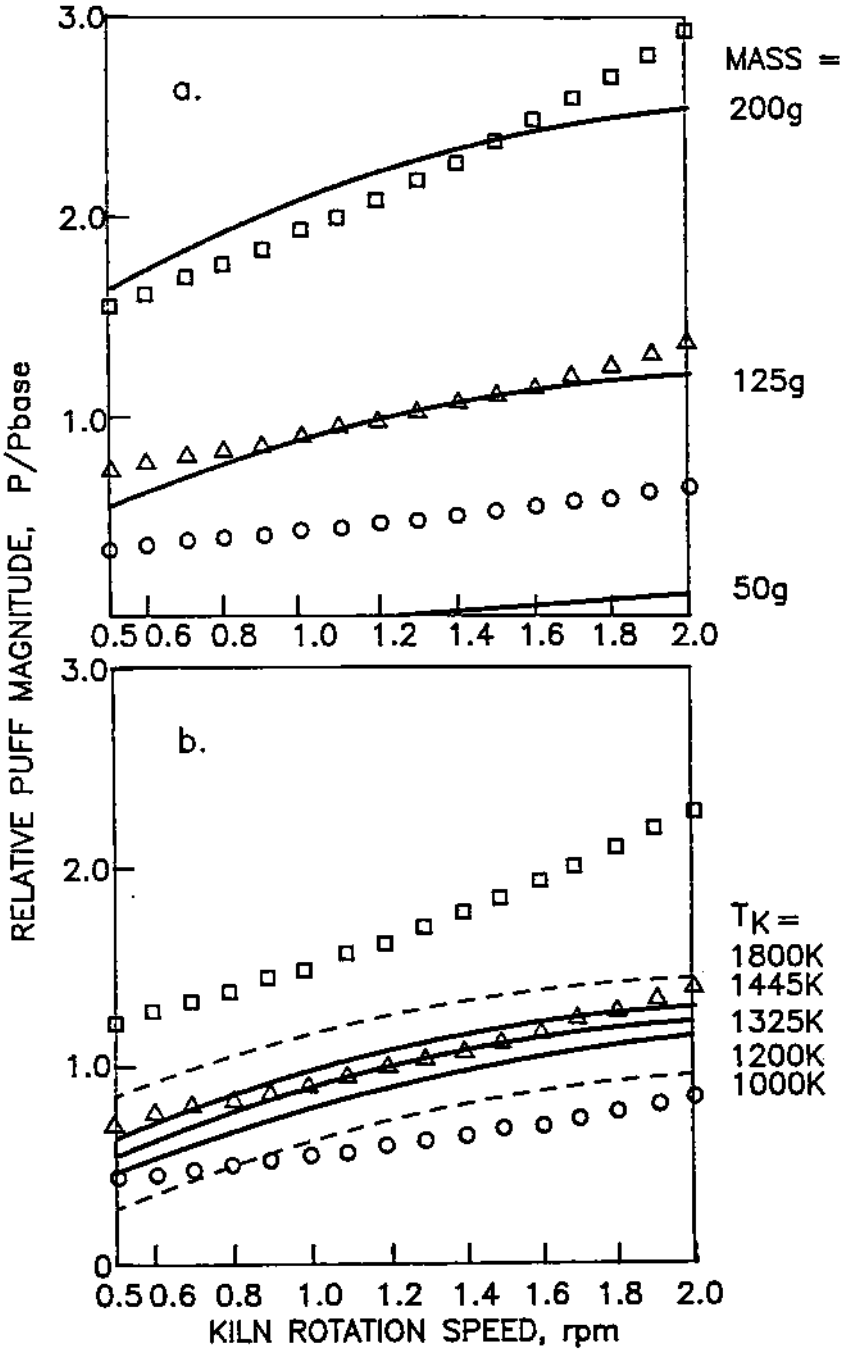

FIGURE 4 Comparison of interpolated data with predicted behavior. Plots present relative toluene puff magnitude (P/P_{base}) versus kiln rotation speed (RPM) for: (a) Variable charge mass at constant kiln temperature (T_K = 1325 K); ○ Interpolated data, MASS = 50 g; △ Interpolated data, MASS = 125 g; □ Interpolated data, MASS = 200 g; ——, predicted by model. (b) Variable kiln temperature at constant charge mass (MASS = 125 g); ○ Interpolated data, T_M = 1088 K, T_K = 1200 K; △ Interpolated data, T_M = 1227 K, T_K = 1325 K; □ Interpolated data, T_M = 1346 K, T_K = 1445 K; ——, – – –, predicted by model.

mass, MASS = 125 g toluene on 135 g sorbent. Symbols denote interpolated data resulting from the statistically derived quadratic model. The following important conclusions can be drawn from the interpolated experimental data depicted on Figure 4:

(a) Puff magnitude increases with increasing charge mass.
(b) Puff magnitude increases with increasing kiln rotation speed.
(c) Puff magnitude increases with increasing kiln temperature.

Additional experiments using a less volatile fuel oil showed also that puff magnitude decreases as liquid volatility decreases. Available full-scale data (Bastian and Wood, 1987; Wood, 1987) from an industrial kiln/afterburner system support our laboratory kiln simulator results concerning the effect of kiln rotation speed, and this provides evidence that the experimental system used here does relate to industrial practice in general.

THEORETICAL MODEL

The shape and duration of the hydrocarbon trace shown on Figure 3a strongly suggest that transport phenomena, and not only vapor pressure driving forces, modulate the evolution of waste material into the bulk gas phase. The strong effect of kiln rotation speed suggests that the rate of mass evolution depends on the rate at which new surface is exposed to the hot kiln environment and that this facet should be included in the model.

Our approach was to formulate an idealized prototype model which, hopefully, correctly describes the salient features present in the practical case, without omitting any physical phenomenon of first order importance. The tumbling motion of the sorbent/waste is extremely complex, and it is not fruitful to attempt to model that in scrupulous detail. Prior approaches (Zablotny, 1965) have focused on prediction of the rate at which a bed is folded over to expose new surface area, but are more valid when the bed comprises a significant volume of the kiln chamber. Other approaches (Kramke and Wilson, 1986a, 1986b) have assumed that particles fall independently of one another, with no particle to particle interaction. Our observations of the behavior of the small amount of sorbent aggregate in the kiln during the evolution of a puff suggested to us that neither of these two approaches properly simulated events occurring in our system, but that an empirical approach based on fragmentation theory not only had the advantage of greater simplicity but might also be more applicable. In contrast to other kiln modeling efforts (Lighty *et al.*, 1987) no effort is made here to model mixing in the gas phase. Rather, we hypothesize that the key phenomena are controlled by the rate of evolution of material from the sorbent aggregate, and compare the consequences of this hypothesis to the data in order to evaluate its validity.

The model proposed here consists of two parts as shown on Figure 5. The first (Figure 5a) couples the prototype problem of transient simultaneous heat and mass transfer in a sorbent aggregate layer, with local vaporization rates depending on local vapor pressure and composition; and the second (Figure 5b) is a fragmentation model, which relates kiln rotation speed to the rate at which new surface area is exposed. The fragmentation model is empirical and therefore does not exclude other fundamental mechanisms which might expose new surface area for mass and heat transport.

Vaporization Model

Consider time dependent, simultaneous heat and mass transfer in a sorbent aggregate, as shown on Figure 5a. The sorbent aggregate is composed of individual sorbent

a. VAPORIZATION MODEL

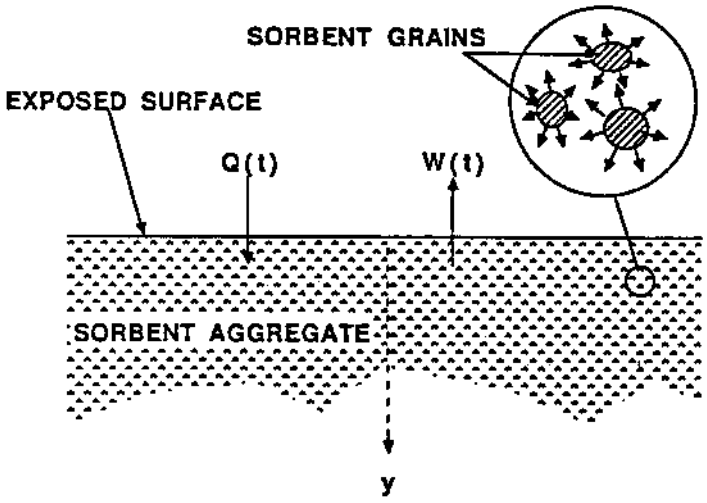

b. FRAGMENTATION MODEL

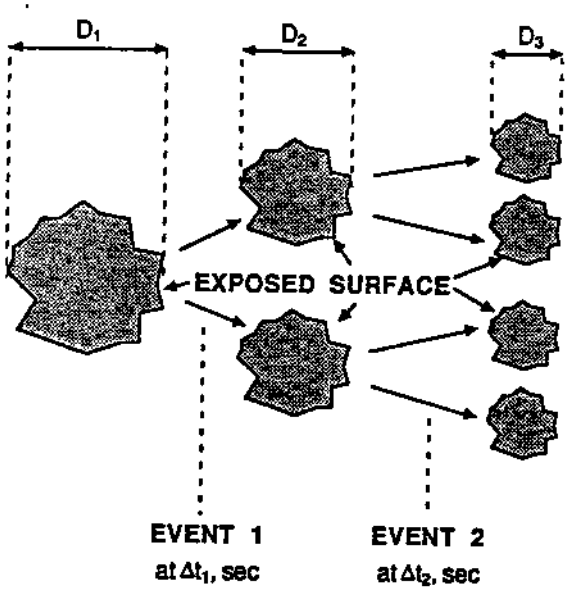

FIGURE 5 Prototype (a) transient vaporization and (b) fragmentation models.

particles, each of which locally releases vapor into the interstitial void volume at a rate determined by the local particle drying rate. The gas evolved diffuses through the voids to the surface, and is released to the kiln environment. The local particle drying rate depends on the local value of the waste vapor pressure, and thus on the local temperature, as determined from the transfer of heat. Equations to be solved are:

Energy:

$$\frac{\partial T}{\partial t} = \frac{k}{(1-\varepsilon)\, C_p \varrho} \frac{\partial^2 T}{\partial y^2} - \frac{\Delta H_v}{C_p \varrho} R_v(C, C_s, T) \tag{1}$$

Species in the interstitial gas phase:

$$\frac{\partial C}{\partial t} = D_{\text{eff}} \frac{\partial^2 C}{\partial y^2} + (1-\varepsilon)\, R_v(C, C_s, T) \tag{2}$$

Species within/on sorbent particles:

$$\frac{\partial C_s}{\partial t} = -R_v(C, C_s, T) \tag{3}$$

Initial and boundary conditions are:

$$\begin{aligned} &t = 0, \quad T = T_0, \quad C = C_0, \quad C_s = C_{s0} \\ &y = 0, \quad T = T_K, \quad C = 0 \\ &y = \infty, \quad T = T_0, \quad C = C_0 \end{aligned} \tag{4}$$

The local vaporization rate, $R_v(t, y)$, is of the form:

$$R_v(C, C_s, T) = \frac{12\, D_m}{d_g^2}\left(\frac{P^{\text{vap}}}{RT}\frac{C_s}{C_{\text{crit}}} - C\right) \tag{5}$$

when C_s is less than C_{crit}; i.e., when the falling rate as used in drying theory is applicable. The Sherwood Number for an individual grain is assumed to be 2, and the Clausius–Clapeyron relationship relates P^{vap} to T. Effective diffusivities are assumed to have the form $D_{\text{eff}} = D_m \cdot \varepsilon^2$ where D_m is the molecular diffusivity (a known function of T) and ε is the interstitial void fraction.

The only completely unknown adjustable parameter is C_{crit}, which defines the onset of the falling drying rate. Because the equations are non-linear and strongly coupled through the steep dependence of vapor pressure on temperature, an analytical solution to obtain:

$$N_A(t)\Big|_{y=0} = -D_{\text{eff}} \frac{\partial C}{\partial y}\Big|_{y=0} \tag{6}$$

as a function of time, and thus the total flux of waste leaving the surface, as a function of time, is difficult. Therefore, the equations were solved numerically, using a fully coupled implicit algorithm and a variable grid (Wendt *et al.*, 1979).

Fragmentation Model

The fragmentation component of the model is based on the assumption that, in a rotary kiln, new surface areas in the sorbent aggregate are exposed through a series of discrete events which can be mathematically represented by fragmentation theory. Following Dunn-Rankin (1987) and Austin *et al.* (1984), it is assumed that the fragmentation rate, $S(D_i, t)$ (*i.e.*, the rate at which particles of size D_i undergo breakage) is given by:

$$S(D_i, t) = k_1(t) \cdot D_i^{k_2} \tag{7}$$

Thus, if k_2 is positive, small particles break up more slowly and last longer than large particles. For our case, we arbitrarily assume that k_1 depends linearly on kiln rotation speed thus:

$$k_1 = k_1' \cdot \text{RPM} \tag{8}$$

which implies that high kiln rotation speeds facilitate particle breakup and new surface exposure. The time interval for which an agregate of size D_i exists is therefore given by:

$$\Delta t_i = 1/(\text{RPM} \cdot k_1' \cdot D_i^{k_2}) \tag{9}$$

We have no idea how many particles each aggregate forms at each fragmentation event. Therefore, we assumed that each event produces two particles out of one, as shown on Figure 5b. Conservation of total volume yields the instantaneous area which increases with time.

This fragmentation model was coupled to the transient vaporization model by calculating, before each event, a new average waste sorbent concentration remaining in the sorbent from the total amount of waste vaporized into the gas phase during the time interval before the break. An average sorbent temperature was also calculated. Thus, after each event, the new aggregates were assumed to have uniform initial concentrations and temperatures, and the transient vaporization model (which quickly generates gradients) was applied again, until the next fragmentation event occurred. This process continued until all the waste originally in the sorbent had evolved.

A puff is assumed to occur when the supply of oxygen from the primary flame is insufficient to completely satisfy the stoichiometric requirement of the waste being evolved. It is calculated as "Unsatisfied Oxygen Demand," thus:

$$Y_{O_2} = Y_{O_2}^0 - \nu \cdot F_w/F_f$$

$$\text{Unsatisfied Oxygen Demand} = 0 \text{ for } Y_{O_2} \geqslant 0 \tag{10}$$

$$\text{Unsatisfied Oxygen Demand} = -Y_{O_2} \text{ for } Y_{O_2} < 0$$

Clearly, according to this definition, puff intensity is proportional to the stoichiometric oxygen requirement of the waste, and inversely proportional to the flow of oxygen from the primary flame.

As shown on Table I, the model contains only three completely unknown parameters, namely C_{crit}, k_1', and k_2. The remaining parameters can be obtained from physical and chemical properties of the sorbent and the waste. The fragmentation parameters,

TABLE I
Waste, sorbent, and kiln parameters used to predict the "base case" puff shape presented in Figure 3c

Waste Parameters (toluene)

MASS	125.0 g
MW	92.0 g/gmole
T_b	383.6 K
ΔH_v	7688.44 cal/gmole
P^{vap} at 298 K	0.05516 atm
P^{vap} at 1325 K	1296.0 atm
Collision diameter	52.7 angstroms
D_m	0.073 30 cm^2/s
ν	0.098 gmole O_2 required/g waste
C_0	2.257E-06 gmole/cm^3
C_{s0}	3.019E-03 gmole/cm^3 sorbent

Sorbent Parameters

Sorbent mass	135.0 g
ϱ	0.3 g/cm^3
k	1.41E-04 cal/s cm K
C_p	0.172 cal/g K
ε	0.5616
d_s	0.5 cm
D_{eff}	0.02312 cm^2/s
C_{crit} (defines falling rate)	0.1 gmole/cm^3 sorbent
Container diameter	8.9 cm
Container length	16.5 cm
k_1'	0.01
k_1	0.0125
k_2	2.0

Assume: Sorbent properties are those of sawdust when corncob properties unavailable. Each aggregate forms two pieces at each fragmentation event.

Kiln Parameters

T_K	1325 K
T_0	298 K
RPM	1.25 rpm
F_f	1.32 gmole/s
$Y^0_{O_2}$	0.097 75

k_1' (yielding k_1) and k_2, were chosen on the basis of yielding predicted transient profiles over time-scales that corresponded to those observed. No attempt was made here to determine "best values" to fit the data, and the model should therefore be considered only as a first step towards the prediction of puff intensities and magnitudes.

MODEL RESULTS

Predicted Transient Puff Shape

Figures 3b and 3c show the predicted temporal profile of the "Unsatisfied Oxygen Demand" for the case representing the experimental puff of Figure 3a and the base case, respectively. The responses on Figures 3b and 3c should be considered to be directly related to puff intensity (assuming excess production of soot does not deplete hydrocarbons), and should be compared to the real-time hydrocarbon measurement

trace shown on Figure 3a. Clearly, there are some differences between predictions and measurement, but there are also many qualitative similarities. First, the duration of the predicted puff is of the same order as that measured. Second, both predictions and measurement show multiple peaks, and this suggests that the model has some validity. Note also that for both measurement and predictions the peak intensity occurs during the middle of the puff. For the base case (Figure 3c) the puff shape corresponded more closely to those measured. In view of difficulties in properly measuring "Unsatisfied Oxygen Demand," and in quantitatively predicting a pseudo-random process such as surface exposure, we think agreement between theory and data is acceptable, at least from a qualitative sense. Comparison between Figures 3b and 3c, however, indicates that predicted puff shape depends strongly on waste and kiln parameters. The waste, sorbent, and kiln parameters used to generate the base case puff (Figure 3c) are presented in Table I (Foley, 1978; Reed, 1978; Weast and Astle, 1982).

Effect of Kiln Parameters

As kiln rotation speed increases, the number of fragmentation events creating new surface area during the puff increases. Areas under these traces were obtained by numerical integration, leading to Figure 4 in which relative puff magnitude is plotted against both kiln rotation speed for variable charge mass (Figure 4a) and variable kiln temperature (Figure 4b). The base case, against which all others were normalized, is the area under the trace on Figure 3c. There is qualitative agreement between model and data. Both show increased puff magnitude as kiln rotation speed, charge mass, and kiln temperature are increased. Experimental effects of temperature were greater than those predicted, although trends are in the correct direction. Note that the current model uses a temperature rather than a heat flux boundary condition for the energy equation. Absolute comparison between data and model could no doubt be improved by including more complex boundary conditions and by proper adjustment of unknown parameters, namely C_{crit} which denotes onset of the falling drying rate, and the fragmentation parameters. The model shows that higher kiln temperatures increase devolatilization because of their effect on vapor pressure, while increasing kiln rotation speed increases the number and frequency of fragmentation events exposing and increasing fresh surface area to the hot kiln environment.

Predicted Profiles within Sorbent

It is instructive to examine the profiles of interstitial gas-phase concentration, C, concentration within sorbent grains, C_s, and temperature, T, within the sorbent aggregate, since these provide insight into how and why the puff is generated. We present profiles for the base case (see Figure 3c) at long times (between 20 and 35 s) during the most rapid (second to last) evolution period.

Figures 6a through 6c show interstitial gas-phase concentration, sorbent concentration, and temperature profiles, respectively, at five times. The gas phase concentration profile peaks near the sorbent boundary, and this peak slowly moves to the inside of, but never more than halfway into, the sorbent aggregate as time progresses. Thus, the semi-infinite model shown on Figure 5a is valid. The temperature profiles are not simply described by the familiar self-similar form because latent heat effects are important. As volatilization rates increase, the temperature drops and the shape of the profile changes dramatically. The sorbent concentration profile is consistent with the other two, and shows the rapid depletion of waste near the aggregate surface, and the increased resistance to mass transfer out of the surface as time progresses.

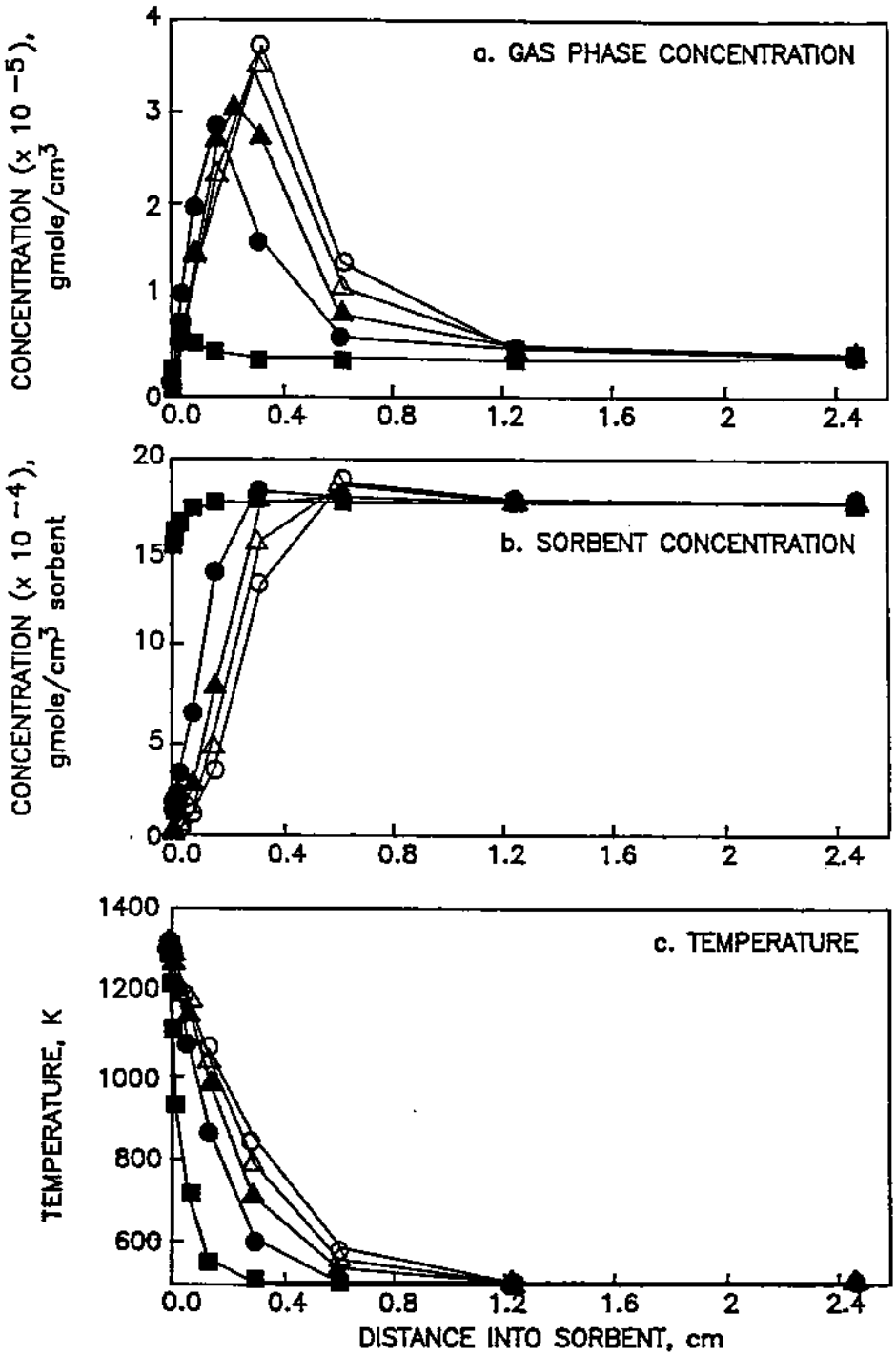

FIGURE 6 Concentration and temperature profiles within sorbent aggregate. (a) Interstitial toluene gas-phase concentration, C; (b) Toluene concentration within sorbent grains, C_s; (c) Temperature, T. Profiles are presented for five times between 20 and 35 seconds and correspond to the second to last transient peak of the "base case" puff shape presented on Figure 3c; ■ 20.75 s, ● 25.0 s, ▲ 28.2 s, △ 31.5 s, ○ 34.2 s.

The model also indicates that the aggregate size, D_i, has decreased to 2.4 cm from an initial value of 8.9 cm because of the number of fragmentation events that have occurred up to this point.

Effect of Waste and Sorbent Parameters

The effect of stoichiometric oxygen requirement (and of the supply of oxygen from the primary flame) is clearly given by Equation 10, and so is not plotted here. This parameter is extremely important in the ranking of wastes insofar as their propensities to form puffs are concerned. Liquid waste mass is also, clearly, of first order importance, as shown on Figure 4a.

Waste mass and stoichiometric oxygen requirement are not the only waste parameters of importance, however, since volatility plays an equally important role. This was observed experimentally when touluene was compared to fuel oil. In the model we considered waste boiling point and latent heat to be correlated using Trouton's Rule:

$$\frac{\Delta H_v}{T_b} \approx 22 \tag{11}$$

and thus reduced the variables describing volatility to one, namely waste normal boiling point. Figure 7 shows the effect of varying normal boiling point, and clearly indicates the importance of this parameter in ranking wastes. Puff intensities became quite weak as normal boiling point was increased.

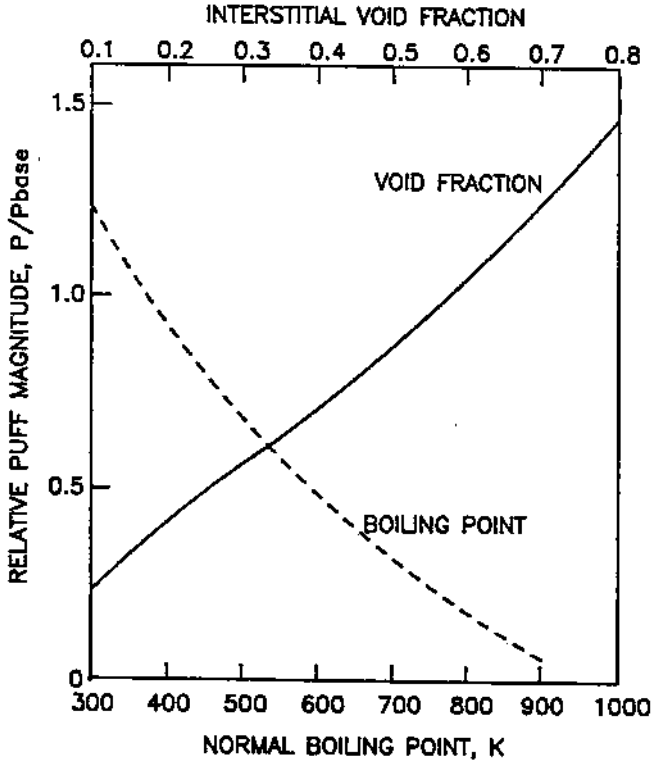

FIGURE 7 Predicted effects of changes in the waste normal boiling point and the interstitial sorbent void fraction on the relative puff magnitude (P/P_{base}).

In the experiments, sorbent amounts and characteristics were not varied. Therefore it is useful to exploit the model to extrapolate outside the test matrix and attempt to predict the effects of sorbent porosity, absorbency, and container volume which are not independent. We define porosity as equal to the volume fraction of the interstitial space between particles, while absorbency relates to the sorption properties within each grain. The effect of changes in porosity, changed by varying the mass of sorbent in a given container, but assuming that the sorbent was uniformly dispersed throughout the container, is shown on Figure 7. If sorbent masses are changed and container volumes are reduced proportionately, keeping porosity the same, the model predicts little effect on the puff magnitude.

CONCLUSIONS

Failure modes occurring during the batch incineration of liquid wastes bound on sorbents are promoted by high kiln rotation speeds and high kiln temperatures. The latter result is contrary to normal incineration practice which is to encourage higher temperatures to achieve higher destruction and removal efficiencies (Oppelt, 1987). Both experimental results, however, are qualitatively supported by an unsteady vaporization/fragmentation model describing the salient features of the dominant processes. The model also indicates that waste mass, waste volatility, and sorbent parameters control the intensity and magnitude of transient puffs. Container dimensions are important only insofar as they affect the bulk porosity of the sorbent.

The developed model shows promise in describing some of the complicated processes occurring in the kiln. It is clearly but a first step in the development of future models which can be used to quantitively predict puffs and to rank wastes. Much more work remains to be done to improve and calibrate the fragmentation portion of the model, to incorporate more realistic boundary conditions in the transport model, and to include some effects of mixing and chemical reactions in the gas phase.

DISCLAIMER

REFERENCES

Austin, L. G., Klimpel, R. R., and Luckie, P. T. (1984). *Process Engineering of Size Reduction: Ball Milling*, Soc. Mining Engrs., New York, NY.

Bastian, R. E. and Wood, R. W. (1987). Eastman Kodak Company Chemical Waste Incineration Organic Compound Destruction, *Proceedings on Rotary Kiln Incineration of Hazardous Waste*, pp. 80, Louisiana State University, Baton Rouge, LA.

Dunn-Rankin, D. (1987). *Kinetic Model for Simulating the Evolution of Particle Size Distributions during Char Combustion*, Sandia Report SAND87-8615.

Foley, K. M. (1978). *Chemical Properties, Physical Properties and Uses of the Andersons' Corncob Products*, 2nd ed., The Andersons, Maumee, OH.

Handbook of Chemistry and Physics, (1982). Weast, R. C. and Astle M. J. eds., 63rd ed., CRC Press Inc.

Hicks, C. R. (1973). *Fundamental Concepts in the Design of Experiments*, 2nd ed., Holt, Rinehart and Winston Inc.

Kramke, F. A. and Wilson, J. B. (1986a), Computer Simulation of a Rotary Dryer, Part I: Retention Time, *AIChE J.* 32(2), 263.

Kramke, F. A. and Wilson, J. B. (1986b). Computer Simulation of a Rotary Dryer, Part II: Heat and Mass Transfer. *AIChE J.* 32(2), 269.

Lighty, J. S., Pershing, D. W., Lemieux, P. M., Silcox, G. D., Owens, W. D., Cundy, V. A. (1987). Thermal Treatment of Solids in a Rotary Kiln Environment. *Proceedings on Rotary Kiln Incineration of Hazardous Waste*. pp. 129. Louisiana State University, Baton Rouge, LA.

Linak, W. P., Kilgroe, J. D., McSorley, J. A., Wendt, J. O. L., and Dunn, J. E. (1987a). On the Occurrence of Transient Puffs in a Rotary Kiln Incinerator Simulator I. Prototype Solid Plastic Wastes, *J. Air Poll. Cont. Assoc.* 37, 54.

Linak, W. P., McSorley, J. A., Wendt, J. O. L., and Dunn, J. E. (1987b). On the Occurrence of Transient Puffs in a Rotary Kiln Incinerator Simulator II. Contained Liquid Wastes on Sorbent, *J. Air Poll., Cont. Assoc.* 37, 934.

Oppelt, E. T. (1987). Incineration of Hazardous Waste A Critical Review., *J. Air Poll. Cont. Assoc.*, 37, 558.

Reed, R. J. (1978). *North American Combustion Handbook*, 2nd ed., North American Manufacturing Co., Cleveland, OH.

Wendt, J. O. L., Martinez, C. M., Lilley, D. M. and Corley, T. L. (1979). Numerical Solution of Stiff Boundary Valued Problems in Kinetics and Diffusion. *Chem. Eng. Sci.* 34, 527.

Wood, R. W. (1987). Eastman Kodak Company Rotary Kiln Performance Testing. *Proceedings on Rotary Kiln Incineration of Hazardous Waste*, pp. 105, Louisiana State University, Baton Rouge, LA.

Zablotny, W. W. (1965). The Movement of the Charge in Rotary Kilns, *J. Intl. Chem. Eng.* 5(2), 360.